Environmental Pollution 363 (2024) 125189

Contents lists available at ScienceDirect

Environmental Pollution

journal homepage: www.elsevier.com/locate/envpol

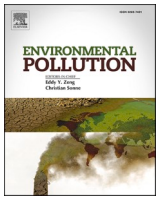

A mechanistic study on the interaction effects between legacy and pollutants of emerging concern: A case study with B[*a*]P and diclofenac☆

Carla Martins [a,b,**], Lara M. Carvalho [c,d], Inês Moutinho Cabral [a,b], Leonor Saúde [c,d], Kristian Dreij [e], Pedro M. Costa [a,b,*]

[a] Associate Laboratory I4HB Institute for Health and Bioeconomy, NOVA School of Science and Technology, NOVA University of Lisbon, 2829-516, Caparica, Portugal
[b] UCIBIO Applied Molecular Biosciences Unit, Department of Life Sciences, NOVA School of Science and Technology, NOVA University of Lisbon, 2829-516, Caparica, Portugal
[c] GIMM - Gulbenkian Institute for Molecular Medicine, 1649-035 Lisboa, Portugal
[d] Faculdade de Medicina, Universidade de Lisboa, 1649-035 Lisboa, Portugal
[e] Institute of Environmental Medicine, Karolinska Institutet, Box 210, SE-171 77 Stockholm, Sweden

ARTICLE INFO

Keywords:
Benzo[*a*]pyrene
NSAID
Mixture
Zebrafish
Transcriptomics
Pathway analysis

ABSTRACT

To study the intricate toxicological mechanisms triggered by exposure to mixed pollutants, we exposed zebrafish embryos to legacy and emerging pollutants through binary mixtures of benzo[*a*]pyrene (B[*a*]P) and diclofenac (DFC). The combination of next-generation transcriptomics and toxicopathology disclosed instances where exposure to mixtures did not attain the expected sum of acute effects of individual toxicants, indicating potential antagonism. Despite overall higher mortality in DFC treatments, the same antagonistic trend was noted in genotoxicity and molecular pathways related to RNA turnover, cell proliferation, apoptosis and cell-cycle control. The formation of oedemas in the heart cavity and yolk sac can be an adverse outcome (AO) resulting from exposure to DFC isolated or combined, whose potential key events (KEs) may involve cell cycle arrest and apoptosis via p53 and MAPK pathways. From the findings it can be hypothesised that, rather than genotoxicity, the molecular initiating event (MIE) maybe inflammation triggered by oxidative stress. Nonetheless, the exact role of ROS in the process needs further clarification. Impaired eye function by action of DFC and B[*a*]P combined may be another AO, in the case caused by ocular degeneration following the suppression of biologic processes and molecular functions involved in eye development and its functionalities, possibly linked to hindered regulation of the expression of *hsf4* and *cryaa*. Altogether, toxicopathology suggests predominance of antagonistic effects, but its integration with mechanism suggests that interactions between DFC and B[*a*]P in environmentally-relevant concentrations that may lead to hindrance of key functions such as the control of inflammation and cell cycle. These outcomes suggest potentially severe implications for health and survival, in case of prolonged chronic exposure to combined toxicants.

1. Introduction

Environmental contamination often involves complex mixtures of legacy and emerging toxicants whose combined effects are difficult to predict. This means that legacy contaminants like carcinogenic polycyclic aromatic compounds (PAHs), which are some of the most ubiquitous pollutants worldwide (Dat and Chang, 2017), often co-occur with pollutants of emerging concern such as pharmaceuticals and derivatives. In the latter case, concentrations in surface waters are increasing, mostly due to inefficient removal by wastewater treatment, to which is added the mounting use of medical and veterinary drugs in both industrialised and developing regions (Arman et al., 2021; Verlicchi et al., 2012; Zhou et al., 2019). Despite the effort to produce regulatory guidelines and safety levels of individual contaminants such as the EU Environmental

☆ This paper has been recommended for acceptance by Dr Mingliang Fang.

* Corresponding author. Egas Moniz Center for Interdisciplinary Research (CiiEM); Egas Moniz School of Health & Science, Campus Universitário, Quinta da Granja, 2829Caparica, Almada, Portugal.

** Corresponding author. Associate Laboratory i4HB Institute for Health and Bioeconomy, NOVA School of Science and Technology, NOVA University of Lisbon, 2829-516 Caparica, Portugal.

E-mail addresses: c.martins@campus.fct.unl.pt (C. Martins), pmcosta@fct.unl.pt (P.M. Costa).

https://doi.org/10.1016/j.envpol.2024.125189
Received 8 July 2024; Received in revised form 9 September 2024; Accepted 22 October 2024
Available online 23 October 2024

Quality Standards (EQSs), it remains challenging to derive risk in realistic scenarios that almost invariably imply chronic exposure to mixed pollutants. Understanding the toxicological mechanism underlying the 'cocktail effect' of pollutant mixtures can thus be pivotal to understand hazard and risk, since toxicological mode-of-action is increasingly acknowledged as key to predict adverse effects (e.g., Cassee et al., 1998; Silins and Högberg, 2011; Vitorino and Costa, 2023). It must be noted that toxicant interaction effects can be complex and categorized as additive, antagonistic or synergistic, depending on their relationship with the mode-of-action of individual chemicals (Hernández et al., 2017). By delivering multiple endpoints in single runs, omics approaches can be used to associate adverse outcomes (AOs), key events (KEs) and upstream molecular initiating evens (MIEs) triggered by exposure to mixtures of pollutants if anchored by toxicopathological traits (see, e.g., Madeira and Costa, 2021; Martins et al., 2019). Consequently, adverse outcome pathways (AOPs), a conceptual framework derived to handle the complexity of environmental risk assessment in ecotoxicology (Ankley et al., 2010), can be derived even in cases where reduced levels of individual toxicants would render difficult to establish causal networks between toxicants and effects, with emphasis on chronic diseases such as cancer (e.g., Hayes et al., 2019; Vitorino and Costa, 2023).

The present work combines the PAH benzo[*a*]pyrene (B[*a*]P), a well-known model carcinogen, as representative of legacy toxicants and the pharmaceutical drug diclofenac (DFC), one of the most widely used non-steroid anti-inflammatory drugs (NSAIDs) worldwide. Zebrafish (*Danio rerio*) was the selected biological model given its versatility as a vertebrate model in aquatic systems and due to the genetic similarity to humans offers toxicological answers in biomedical field, establishing the bridge between contamination and consequences in human health and wildlife (Ablain and Zon, 2013; Chahardehi et al., 2020; Howe et al., 2013). In the EU, DFC is listed as a 'pollutant of emerging concern', whereas B[*a*]P is long acknowledged as priority pollutant, with an Environmental Quality Standard (EQS) set at 0.05 μg/L (Directive, 2008/105/EC), now reviewed to 1.70×10^{-4} μg/L (Directive, 2013/39/EU). This carcinogen has been estimated to be responsible for about 400 new cases of lung cancer per year in Europe alone as a result of inhalation (Guerreiro et al., 2016). Despite the scant literature specifically focusing on the co-occurrence and combined risk of legacy and emerging pollutants in natural environments, the two toxicants commonly exceed EQS in European surface waters, inclusively simultaneously, as reported by Vystavna et al. (2018) in three Ukrainian urbanised rivers.

Like most PAHs, B[*a*]P results from incomplete combustion of organic materials, from fuels to cigarettes and it is a potent mutagen through the formation of bulky adducts between its CYP1A/B bioactivated metabolites (especially diol epoxides) with DNA (see for instance Boström et al., 2002; Costa, 2022). The toxicant can promote proliferation of neoplastic cells via mutation in certain regions of the genome, leading to the expression of oncogenes like *ras*, plus the transcriptional suppression of tumour suppressor genes (especially p53), and also through activation of pro-inflammatory cytokines (Denissenko et al., 1996; Ross and Nesnow, 1999). In turn, DFC, which is broadly used in human and livestock health, has an EQS of 0.1 μg/L and in 2015 was integrated in the 1st Watch List for substances in surface waters for continuous monitoring by the Commission Implementing Decision (EU) 2015/495, due to its high risk for wildlife, aquatic animals included (Oaks et al., 2004; Diniz et al., 2015; Parolini, 2020). This drug, which controls inflammation by inhibiting the activity of cyclooxygenase family members COX-1 and COX-2 thus disrupting the prostaglandin pathway (Gan, 2010), is chiefly eliminated via glucuronidation. Nonetheless, it can also be metabolized by cytochrome P450 members (CYP), especially CYP2C and CYP3A, the latter of which is responsible for generating the most reactive metabolites (Leemann et al., 1993). Indeed, several DFC derivatives were linked to mechanisms of hepatotoxicity associated to oxidative stress and mitochondrial dysfunction (Inoue et al., 2004). Interestingly, DFC has been suggested to hold anti-cancer proprieties by interfering with angiogenesis and cytokine signalling, but the full mechanism has not yet been described (Arisan et al., 2018; Duval et al., 2019; Kaur and Sanyal, 2011).

Besides the environmental relevance of B[*a*]P and DFC, these pollutants share metabolization via CYPs and can hypothetically interact through pathways related to inflammation and cell pre-neoplastic processes. However, interaction mechanisms and downstream effects remain, at the current stage, conjectural. The present work aimed primarily at investigating a possible mechanistic network for the interaction between these two model toxicants in vertebrates at environmentally-relevant concentrations, potentially hinting at novel adverse outcomes that can be investigated for application in risk assessment strategies.

2. Methods

2.1. Chemicals

Benzo[*a*]pyrene (CAS: 50-32-8) was acquired from TCI EUROPE (Zwijndrecht, Belgium) and diclofenac sodium (CAS: 15,307-79-6) from Acros organics (Geel, Belgium). Stock solutions of B[*a*]P (0.4 and 4 mM) and DFC (3.1 and 31.4 mM) were prepared in dimethyl sulfoxide (DMSO) and sterilised ultrapure water, respectively.

2.2. Test organisms

Zebrafish embryos were obtained from adult wildtype *Danio rerio* (AB incross) maintained in a six-rack recirculating system (Tecniplast, Buguggiate, Italy) equipped with a reverse osmosis unit, under controlled conditions, namely conductivity set at 800 μS, pH 7.0, at 28 °C on a 14 h light/10 h dark cycle. Animals were fed daily with ZEBRAFEED and *Artemia* (ZM Systems, Winchester, UK). Eggs were collected from multiple couples at early morning hours. Two hours post-fertilisation (hpf), viable eggs were dechorionated mechanically using tweezers as in Henn and Braunbeck (2011). Before exposure, dechorionated eggs (4 hpf) were randomly divided by glass Petri dishes with embryo medium (distilled water supplemented with NaCl, KCl, $CaCl_2$ and $MgSO_4$). During all assays, embryos were placed in an incubator at 28 °C and 90% of the medium was changed with fresh spiked (contaminated), control (vehicles only) or blank (medium only) medium every 24 h.

2.3. Acute toxicity

Acute toxicity bioassays were conducted to assess mortality plus developmental and toxicopathological alterations in zebrafish exposed to toxicants or mixtures between sphere (4 hpf) to early larva (96 hpf) stages, following standard OECD (2013) guidelines, with some adaptations. In brief: the assays were performed with dechorionated eggs that were placed in glass Petri dishes with 10 mL of medium (including vehicle and drug) for 96 h. Each experimental condition held ten embryos ($n = 10$) and was performed in duplicate. The entire experimental set-up was replicated four times. The concentration of DMSO in medium was restrained at $< 0.1\%$ v/v, as recommended by Maes et al. (2012). Individual toxicant concentrations and corresponding binary mixtures were tested, plus control (i.e., spiking with vehicle only) and blank (see Table S1 in Supplementary Information for further details).

The selection of test concentrations was based on realistic thresholds reported in available literature (Table S1). The two lowest B[*a*]P and DFC concentrations were defined in accordance with the EU EQSs (Directives, 2008/105/EC and 2013/39/EU) and the highest concentrations recorded in the environment in EU surface waters (refer to Heberer, 2002; Manoli and Samara, 1999; Gonzalez-Rey and Bebianno, 2014). High concentrations of B[*a*]P tested in acute assays were primarily based on the 8.9 μg/L (4.0×10^{-2} μM) threshold indicated as able to disturb the development the central nervous system in the zebrafish,

with consequent neurodegenerative syndromes in adults (D. Gao et al., 2017). The highest concentration of B[*a*]P was set at 89 μg/L (0.4 μM), corresponding to 1/10 no observed adverse effect level (NOAEL), as defined by Knecht et al. (2017), which falls within the range of maximum concentration of total PAHs (0.0598 μg/L - 127.7 μg/L) measured in highly impacted rivers (Wu et al., 2021). In turn, the highest concentrations of DFC were set using as reference the no observed effect concentration (NOEC) for zebrafish embryos (Ferrari et al., 2003), more specifically 1/5 NOEC 800 μg/L (2.5 μM), 1/10 NOEC 400 μg/L (1.3 μM) and 1/50 NOEC 80 μg/L (0.3 μM). The highest DFC concentration (800 μg/L) follows the highest recorded level of DFC (836 μg/L) found in rives, in the case adjacent to a wastewater effluent (Ashfaq et al., 2017).

Mortality, developmental malformations (lack of somite formation, lack of detachment of the tail-bud from the yolk sac, lack of heartbeat and abnormal pigmentation) and toxicopathological traits (e.g., spinal deformations, oedemas and small eye/blindness) were scored after 24 h, 48 h, 72 h and 96 h of exposure. The scores of developmental malformations and toxicopathological traits were combined into the single variable 'pathological alterations'. Micrographs of surviving embryos after 96 h of exposure were obtained using a DM 2500 LED model microscope equipped with a MC 190 HD camera (Leica Microsystems, Wetzlar, Germany).

2.4. Histopathology

After 96 h of exposure, surviving embryos were fixed in 2.5% v/v glutaraldehyde in 0.1 M Sorensen's phosphate-buffered saline (PBS) pH 7.4, for c.a. 2 h. Samples were then washed in PBS (3 × 10 min) and post–fixed in 1% m/v osmium tetroxide in PBS, in the dark, o/n (all at room temperature). Samples were dehydrated in a progressive series of acetone (30–100%) and embedded in Epon (Sigma-Aldrich, St. Louis, MO, USA), according to Luft (1961). Intermediate infiltration was done using Polypropylene oxide. Sections (2 μm) were produced using a RM 2125 RTS rotary microtome (Leica Biosystems) equipped with a tungsten carbide blade and stained with Toluidine Blue. Scoring was performed using the equipment referenced above.

2.5. Genotoxicity assessment

Genotoxicity was inferred from DNA strand damage using the alkaline Comet assay (Singh et al., 1988), adapted by Martins and Costa (2020) for zebrafish embryos. Embryos were subjected to 48-h bioassays conducted with non-lethal concentrations, i.e., B[*a*]P 0.4 μM (89 μg/L) and DFC 2.5 μM (800 μg/L), as described above. At the end of the assays, ten embryos from each of the three replicates were placed in 100 μL cold (4 °C) Dulbecco's PBS, pH 7.4 and gently minced with pliers before resuspending cells through soft pipetting, which was followed by low-speed centrifuging (250×*g*) at 4 °C (2 min) to remove cellular debris. The fresh supernatant was promptly collected to new tubes to prevent the damage by nucleases and other enzymes in the pellet. The supernatant was embedded in molten (37–40 °C) 1% m/v low melting point agarose (LMPA) prepared in PBS, which was then placed on dried slides pre-coated with 1.2% m/v high melting point agarose (HMPA) prepared in TAE and covered with a coverslip until solidification. Two slides were prepared per sample. The slides were afterwards immersed for 1 h in cold lysis buffer (2.64% m/v NaCl, 3.72% m/v EDTA and 5 mM Tris, pH 10) supplemented with 10% v/v DMSO and 1% v/v Triton-X100, in the dark. Slides then transferred to cold electrophoresis buffer (1 mM EDTA and 300 mM NaOH, pH 13) during 40 min to allow unwinding of DNA and enhance the expression of alkali-labile sites. Electrophoresis was run for 30 min at 25 V, in cold (4 °C) and dark conditions, using the CSL-COM20 Comet Assay Tank (Cleaver Scientific), followed by neutralization in cold 0.1 M Tris-HCL buffer (pH 7.5) for 15 min. Slides were stained with GreenSafe Premium (Nzytech, Lisbon, Portugal) during 10 min in the dark, at room temperature. Comet fields were photographed using the microscope referenced above equipped with a using an EL6000 UV source (also from Leica Microsystems). Scoring was done using CometScore (TriTek Corp, Sumerduck, VA, USA). The mean % DNA in tail (from ≈100 nucleoids per slide) was employed as metric (Azqueta and Collins, 2013). Quality assessment was primarily assessed through the unimodal distribution of nucleoids per five classes of % DNA in tail (0–20% up to 80–100%), which is indicative of negligible interference of cell death.

2.6. Statistics

Statistical analyses were computed with R (Ihaka and Gentleman, 1996). The significance level α was set at 0.05 for all analyses. Data were checked for normality and homogeneity of variances using Shapiro-Wilk's and Levene's Tests, respectively. Parametric data were analysed using *F* test-based ANOVA followed by Tukey's Honest Significant Difference (HSD) test for post-hoc comparisons. Following invalidation of at least one assumption, non-parametric statistics were employed, namely the Kruskal-Wallis ANOVA-by-Ranks H, followed by Dunn's test for multiple comparations. The non-parametric Mann-Whitney *U* test for two-sample comparisons and Spearman's correlation R statistics were also employed.

Due to zero-inflated discrete data for mortality and pathological scoring hindering logistic regression to estimate EC_{50} thresholds, results were analysed through analysis of variance (ANOVA) using generalised linear models (GLM) through a Poisson regression with log link taking B[*a*]P and DFC concentrations plus exposure time as categorial predictors (McCullagh and Nelder, 1989). The significance of explanatory variables was then analysed through deviance analysis by sequential variable addition and χ^2 tests. The model was validated by randomness and normality of standardised Pearson residuals plus Cook's *h* statistic for biasing. Principal component analysis (PCA) based on Pearson's *r* was employed as reduction statistics to ascertain the interlink over time between drug concentrations, mortality and pathological alterations.

2.7. RNA-Seq

Total RNA was extracted from embryos subjected to a third series of bioassays performed under the same conditions and chemical concentrations as those for genotoxicity assessment (0.4 μM B[*a*]P, 2.5 μM DFC and their mixture). After the 48-h exposure, the embryos were collected, pooled per experimental replicate, infiltrated with RNA Later (Qiagen, Hilden, Germany) and stored at −80 °C until further processing. Extraction was done using the RNeasy Protect Mini Kit (Qiagen, Hilden, Germany) following manufacturer instructions. Contaminant DNA was digested in-column with DNase I (RNase-free DNase set from Qiagen) during 15 min at room temperature. Elution was done in 25 μL RNase-free water. Quality and concentration were first analysed using a Nanodrop 1000 spectrophotometer (Thermo Fisher Scientific, Wilmington, DE, USA). Samples were stored at −80 °C until further analyses. The RNA integrity number (RIN) for each sample was determined in an Agilent 2100 Bioanalyzer (Agilent Technologies, Santa Clara, CA, USA), with all samples being found within suitable parameters, i.e., intact or partially degraded samples with RIN ≥7, input of ≥1 μg total RNA, free of contaminating DNA (Schroeder et al., 2006). Library preparation was done using Kapa Stranded mRNA Library Preparation Kit and the generated RNA fragments were sequenced in an Illumina HiSeq 4000 platform, using 150bp paired-end sequencing reads at the scale of 40 M reads.

Reads were mapped against the *D. rerio* reference transcriptome of (Ensembl v99, GRCz11) using Kallisto (Bray et al., 2016), followed by gene expression analyses in R. Expression analyses was conducted using packages edgeR (McCarthy et al., 2012; Robinson et al., 2009) and limma (Ritchie et al., 2015). Gene ontology (GO) and gene enrichment (GE) analyses through GO term analyses and contrasting against the KEGG (Kyoto Encyclopaedia of Genes and Genomes) database were also

performed with R, using packages Biomart (Durinck et al., 2009), org. Dr.eg.db (Carlson, 2019) and multiGSEA (Canzler and Hackermüller, 2020). Pathway analysis was performed through the FGSEA (fast gene set enrichment analysis) test applied to all genes to increase sensitivity and specificity, whereas exploratory GO statistics were based on the Fisher test on differentially-expressed genes (DEGs) in each treatment. In GO/GE analysis, functional enrichments with an adjusted p-value (FDR) < 0.05 were considered significant. Additionally, STRING (Szklarczyk et al., 2019) provided a simulation of protein-protein interaction networks (high confidence was set at 0.74).

2.8. Validation of RNA-Seq data

Experimental validation was achieved by quantitative reverse-transcription PCR (qRT-PCR). The cDNAs were produced from total RNA using the NZY First-Strand cDNA Synthesis Kit (NZYTech, Lisbon, Portugal) as per manufacturer instructions. Specific primers for *cyp1a1*, *hsp70l* toxicity response genes and the housekeeping genes *EF1a* and *18S* were designed using MEGA (Kumar et al., 2018) and Primer-BLAST (see Table S2 in Supplementary Information). After resolving PCR products by gel electrophoresis following amplification using a Biometra 96 thermocycler (Analytik Jena, Jena, Germany) and confirmation by

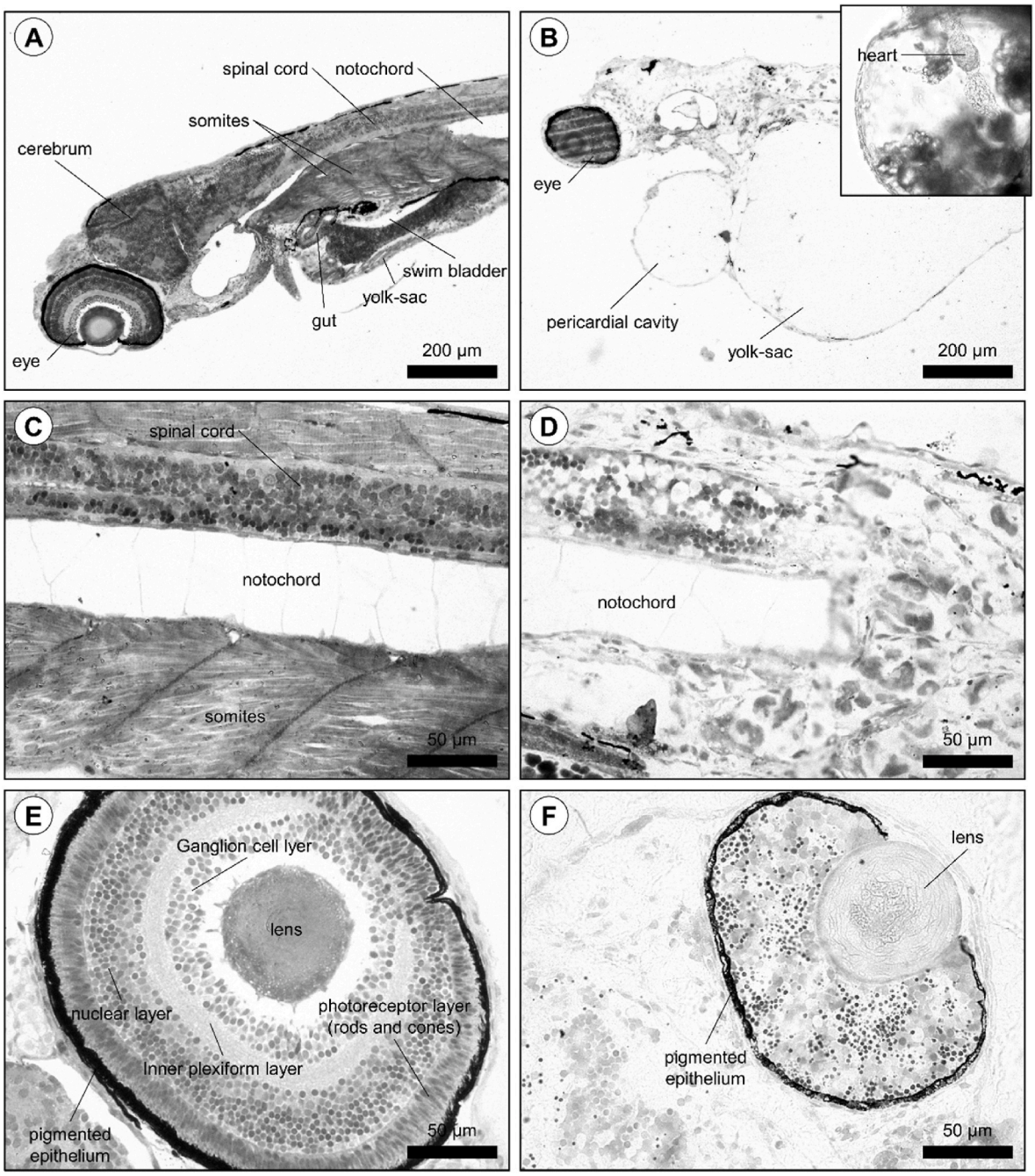

Fig. 1. Examples of histopathological alterations in exposed zebrafish embryos (96 hpf). A) Normal microanatomy observed in a control embryo. B) Embryo subjected to the mixture of highest concentrations of B[*a*]P and DFC (0.4 µM B[*a*]P + 2.5 µM DFC), showing pericardial cavity and yolk-sac oedemas. *Inset:* Detail of heart amidst an oedema (embryo exposed to highest concentration of DFC (2.5 µM). C) Detail of normal somites and notochord from a control embryo. D) Absence of somite formation in embryos exposed to mixture (0.4 µM B[*a*]P + 2.5 µM DFC) E) Normal eye in a control embryo. F) Eye of an embryo exposed to 2.5 µM DFC presenting serious malformations. Toluidine blue staining of epoxy resin sections.

Sanger sequencing, expression was quantified using a Corbett Rotor-Gene 6000 thermal cycler (Qiagen, Hilden, Germany) with the NZY qPCR Green Master Mix (NZYTech). The qRT-PCR programme (50 cycles) was set as: denaturation (94 °C, 45s), annealing (52 °C, 35s) and extension (72 °C, 30s). Primer melting analysis was also conducted to verify specificity of hybridisation. Expression was quantified by the ΔΔCt method (Livak and Schmittgen, 2001). The results were statistically validated by applying the *F* test-based ANOVA followed by Tukey's Honest Significant Difference (HSD) test for post-hoc comparisons between control and treatments gene expression for *cyp1a* and *hsp70l* genes.

3. Results

3.1. Acute toxicity and genotoxicity of DFC, B[a]P and their binary mixtures

Embryos exposed to the highest DFC concentration (2.5 μM), individual or combined, yielded the highest mortality rate, increasing 4-fold between 48 h and 96 h of exposure. Also, the number of embryos with pathological alterations in these treatments tripled after 48 h of exposure (Fig. S1A). Histopathological alterations at 96 hpf were mostly found in zebrafish embryos exposed to the highest DFC concentrations, both individually (1.3 μM and 2.5 μM) and in combination with B[*a*]P, with the embryos having a normal development in the remaining treatments (Fig. 1A). Common histopathological alterations were oedemas in the pericardial cavity and yolk-sac (Fig. 1B), but the heart was mostly unaffected (Fig. 1B, *Inset*) despite seemingly decreased heartbeat and blood flow (not shown). In addition, whereas control embryos presented normal tails and all the properly-formed thirty somite pairs along the notochord (Fig. 1C), embryos exposed to any treatment with highest DFC concentrations (1.3 μM and 2.5 μM) yielded complete absence of somite formation and evidence for muscle degeneration (Fig. 1D), accompanied by severe spinal curvature (scoliosis). These embryos also revealed ocular degeneration (compare Fig. 1E and F). In general, eyes presented normal development at 24 h regardless of experimental conditions, which should indicate that most ocular alterations may be toxicopathological rather than developmental. Loss of retinal melanin pigmentation was noticeable 48 h onwards. At 96 h, retina and lens exhibited severe degeneration (Fig. 1F).

Generalised liner model analyses of mortality (Table 1 and Fig. S2) and pathological alterations (Table 2 and Fig. S3) revealed that DFC concentration and exposure time were the variables with highest influence in both endpoints. This was further supported by the positive link between DFC concentration, mortality and alteration rates after 48 h (Fig. 2A and B). The global correlation (conjoining all treatments and exposure times) between mortality and alteration rates was weak (Spearman's $R = 0.243$, $p = 1.1 \times 10^{-15}$), which was further highlighted by PCA analyses (Fig. 2C and D).

Table 1
Generalised linear model (GLM) for mortality. The significance of each predictor (explanatory variable) was assessed by deviance analysis and ANOVA chi-square test.

Coefficients	Deviance	Resid. Df	Resid. Dev	p	
Exposure time (h)	14.86	1182	2341.3	0.0001161	***
[B[a]P]	15.37	1181	2325.9	8.83×10^{-5}	***
[DFC]	389.39	1180	1936.5	$<2.20 \times 10^{-16}$	***
Exposure time (h): [B[a]P]	0.2	1179	1936.3	0.6559287	
Exposure time (h): [DFC]	550.9	1178	1385.5	$<2.20 \times 10^{-16}$	***
[B[a]P]: [DFC]	0.71	1177	1384.8	0.4006577	
Exposure time (h): [B[a]P]: [DFC]	2.49	1176	1382.3	0.1149048	

Significance levels: (***) 0.001; (**) 0.01; (*) 0.05; (.) 0.1.

Table 2
Generalised linear model (GLM) for pathological alterations. The significance of each predictor (explanatory variable) was assessed by deviance analysis and ANOVA based on the chi-square test.

Coefficients	Deviance	*Resid. df*	*Residual dev.*	p	
Exposure time (h)	16.50	1182	2137.9	4.86×10^{-5}	***
[B[a]P]	3.44	1181	2134.4	0.0637507	.
[DFC]	1063.30	1180	1071.2	$<2.20 \times 10^{-16}$	***
Exposure time (h): [B[a]P]	0.09	1179	1071.1	0.7634414	
Exposure time (h): [DFC]	11.63	1178	1059.4	0.0006496	***
[B[a]P]: [DFC]	0.61	1177	1058.8	0.4334506	
Exposure time (h): [B[a]P]: [DFC]	0.45	1176	1058.4	0.5006677	

Significance levels: (***) < 0.001; (**) < 0.01; (*) < 0.05; (.) < 0.1.

Genotoxicity was found to be significantly influenced by B[*a*]P concentration, in contrast mortality and pathological alteration rates, which were mostly influenced by DFC concentration. The induction of DNA damage was highest in zebrafish embryos subjected to mixture (DFC 2.5 μM + B[*a*]P 0.4 μM) and B[*a*]P-only (0.4 μM) treatments when compared to control (Fig. 3A). Altogether, B[*a*]P-only treatment yielded the highest average frequency of nucleoids in classes 3 (40–60%) and 4 (60–80%) of % DNA in tail comparatively to control (Fig. 3B).

3.2. Inferring toxicological mode-of-action of DFC and B[a]P mixtures from gene expression profiles

Transcriptomic analysis unveiled differences between global gene expression profiles in embryos exposed to either chemical or their combination, relatively to controls, including genes *cyp1a* (Fig. 4A) and *hsp70l* (Fig. 4B), which were analysed by qRT-PCR for validation. In total, exposure to DFC (2.5 μM), B[*a*]P (0.4 μM) plus their mixture (B[*a*]P 0.4 μM + DFC 2.5 μM), yielded about 1300 DEGs, with ~300 genes being differentially expressed in the mixture treatment only (Fig. 4C). Individual B[*a*]P (0.4 μM) treatment unveiled the lowest number of DEGs (30), relatively to control, with only nine genes exclusive of this treatment.

The top five DEGs were generally distinct between treatments, with few exceptions (Table S3), such as the as *pou3f1* gene (involved in brain development and embryonic morphogenesis), which was found to be overexpressed in all three treatments. Mixture and DFC-only treatments also shared two underexpressed genes, *cuedc1a* and *ddb2*, linked to DNA repair and protein ubiquitination. Embryos exposed to the mixture also revealed genes connected to stress response (*hsp70* and *hsp70l*) and RNA binding (*rpl21*) among top five overexpressed, plus underexpressed genes associated to transcription (*znf143b*), translation (*eif2b2*) and glutathione metabolism (*gstr*). In turn, the top five overexpressed genes in DFC treatment were connected to immune and heat shock responses (*ier5* and *ptmaa*), transcription and translation initiation (*btf3* and *rpl32*). The remaining top five underexpressed genes in embryos subjected to isolated DFC were involved in neuronal development (*mbpa*) and lipid metabolism (*apoa4b.2*). In contrast, embryos exposed to B[*a*]P showed more exclusive top five genes. This included the overexpression of genes were related to regulation of RNA polymerase II activity (*med6*), DNA damage response (*ints7*), muscle differentiation (*myog*) and xenobiotic metabolization, including cytochrome P450 1A (*cyp1a*). To these are added underexpressed genes involved in heme biosynthesis (*alad*), glycogen metabolism regulation (*ppp1r3ca*), cellular response against oxidative stress (*rpe*) plus cell proliferation (*CU207215.1*, activator of AKT family member).

Pathway analyses based on GO terms and GE through the KEGG database for zebrafish yielded several significantly altered canonical

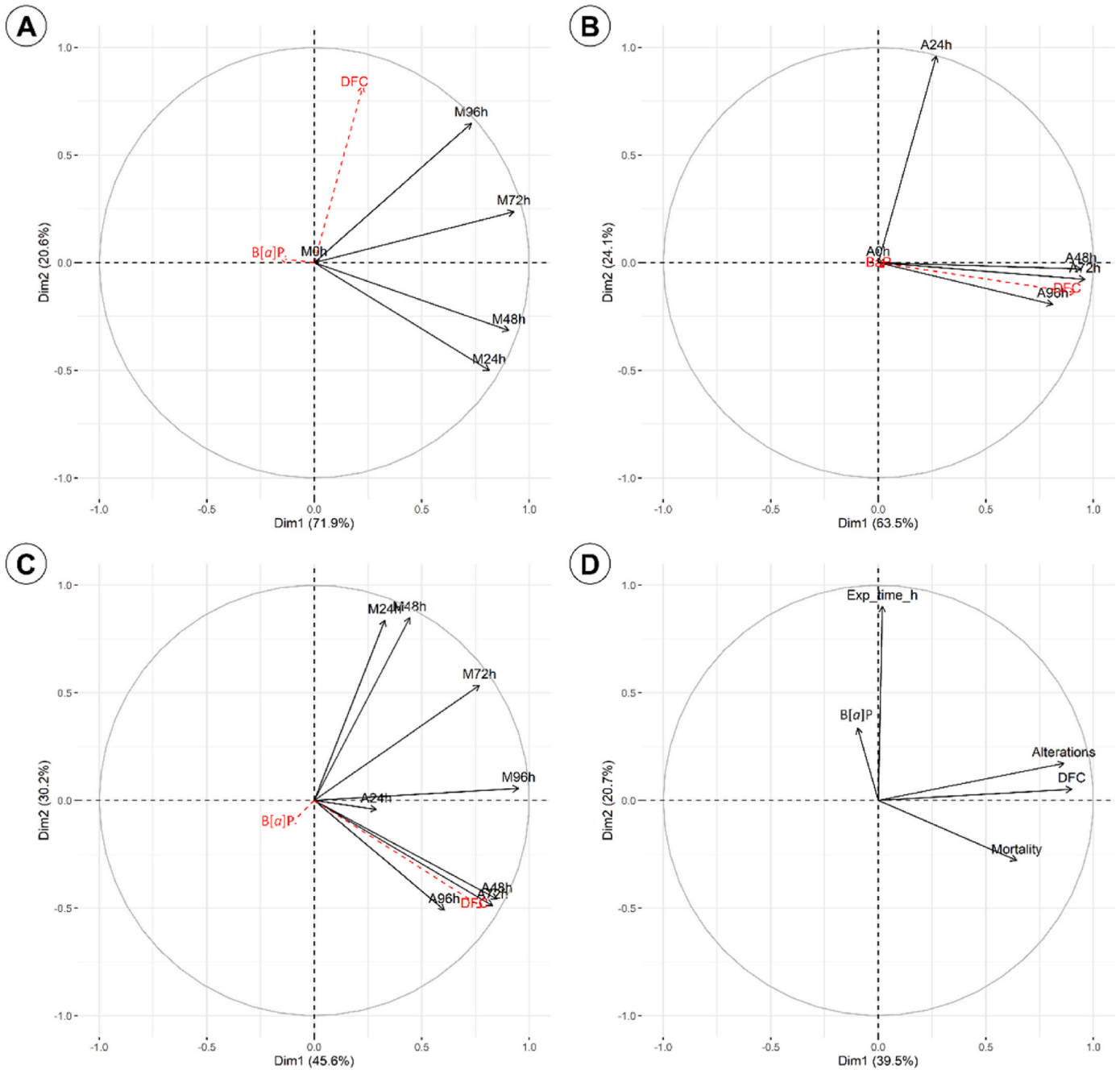

Fig. 2. Principal component analysis (PCA) plots highlighting the relationships between mortality and pathological alteration rates (toxicopathological or developmental) in zebrafish embryos exposed to B[*a*]P, DFC or their mixtures. A) Mortality at different time points (M24h to M96h) contrasted against B[*a*]P and DFC concentrations as supplementary variables. B) Same as previous panel for combined embryo pathological alterations at the different time points (A24h to A96h). C) PCA combining mortality and pathological alterations. D) Analysis combining all variables (mortality and pathological alteration rates; B[*a*]P and DFC concentrations and exposure time).

pathways and GO terms in embryos exposed to the mixture (B[*a*]P 0.4 μM + DFC 2.5 μM), and DFC-only (2.5 μM). Three significantly enriched KEGG pathways (FDR-adjusted $p < 0.05$) were found in embryos subjected to the B[*a*]P (0.4 μM) treatment (Table 3), although without any significant individual GO term (Fig. S4). Canonical pathways were mainly connected with xenobiotic biotransformation, including metabolization by CYPs. Contrarily, embryos exposed to DFC yielded thirteen significantly-enriched KEGG pathways (FDR-adjusted $p < 0.05$). These were mostly related to RNA degradation, apoptosis, cell proliferation and cell cycle regulation, of which we highlight the MAPK, p53, VEGF and FoxO signalling pathways (Table 3). Altogether, GO/GE analysis indicated significant induction of biological processes linked to immune response, DNA replication and transcription, plus suppression of 'ion transport' and 'chemical synaptic transmission' (see Fig. S3).

The mixture treatment revealed alterations in nine significantly-enriched KEGG pathways that essentially amalgamated the pathways indicated above concerning B[*a*]P- and DFC-only treatments. However, several molecular pathways linked to RNA degradation, cell proliferation, apoptosis and cell-cycle control lost their relative enrichment significance when compared to single-exposure treatments (Table 3). In general, most GO terms retrieved from the mixture treatment were common to the DFC-only experiment and essentially associated to

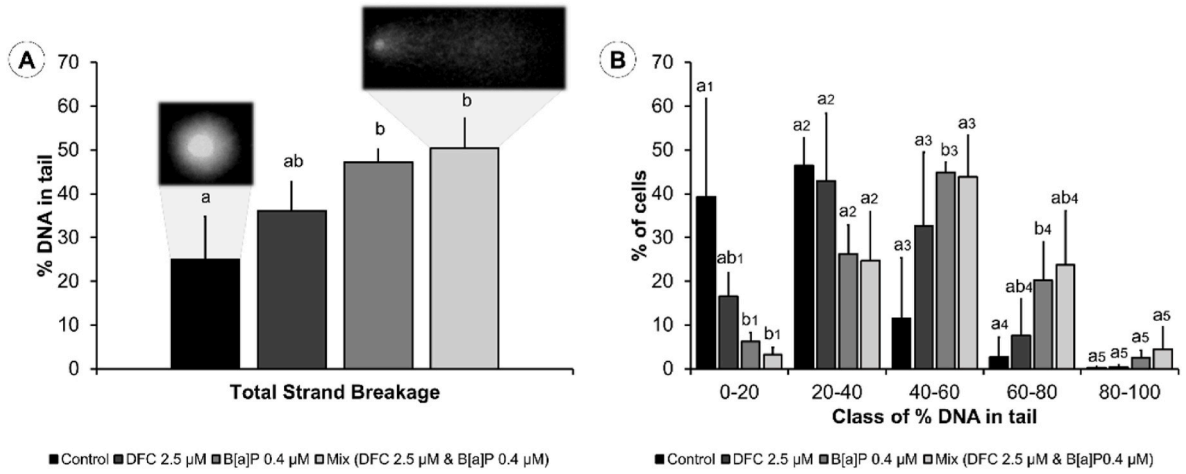

Fig. 3. Damage to DNA (measured through the Comet assay) in zebrafish embryos exposed to B[*a*]P, DFC or their mixture in sublethal concentrations for 48 h. A) Percentage of DNA in Tail as damage metric. Different letters indicate significant differences between treatments (Tukey's HSD test, $p < 0.05$). B) Relative frequency of nucleoids per class of % DNA in tail (given in percentage of nucleoids per class). Different letters indicate significant differences within each class (Dunn's test, $p < 0.05$).

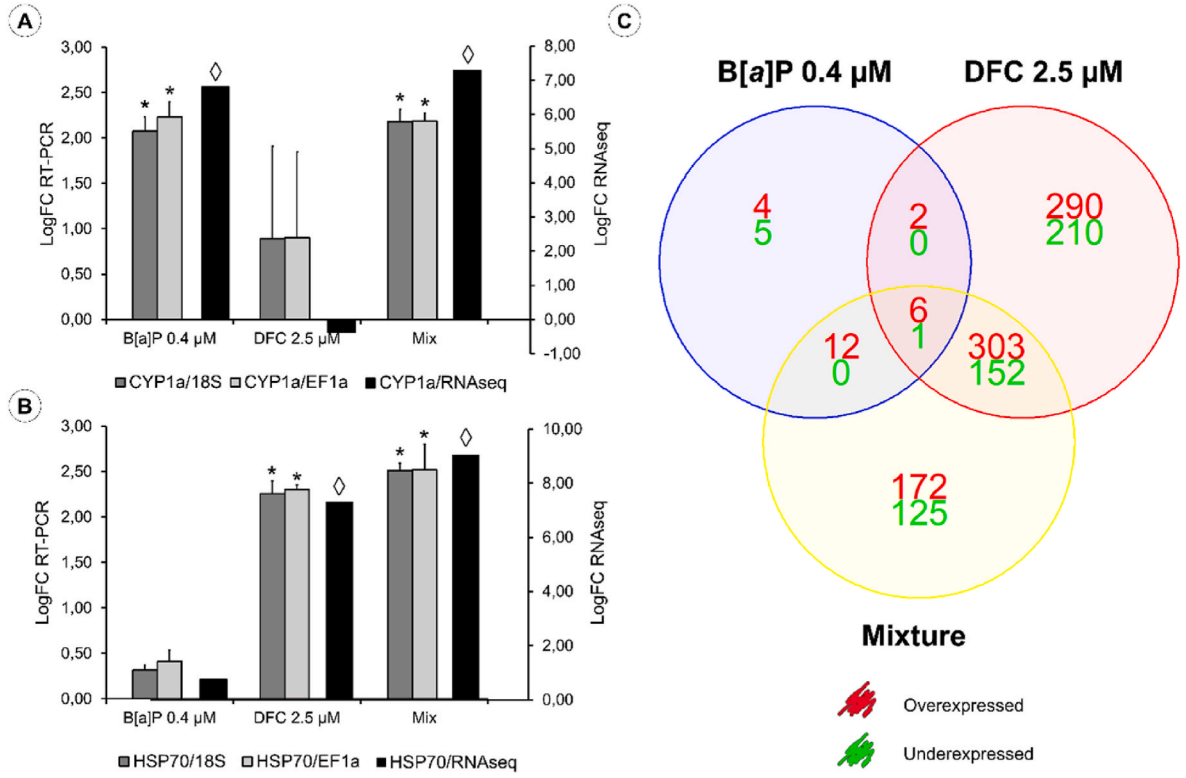

Fig. 4. Summary of RNA-Seq – based transcriptomics analyses in zebrafish embryos exposed to B[*a*]P, DFC or their mixture. Validation of data was provided by comparing CYP1a (A) and HSP70 (B) gene expression between treatments by qRT-PCR and RNA-Seq counts. The symbols indicate significant differences between treatments (Tukey's HSD test, $p < 0.05$). C) Venn diagram illustrating the distribution of overexpressed and underexpressed genes relative to control (RNA-Seq).

regulation of transcription by RNA polymerase II and ion transport (Fig. S5). Interestingly, 'lens development in camera-type eye' and 'visual perception' were GO terms within biological processes exclusively affected by exposure to the mixture treatment. In addition, under the molecular function named potentiation of 'protein heterodimerization activity' and suppression of 'structural constituent of eye lens' were also exclusive to the mixture treatment (Fig. S5).

Protein-protein interactions inferred using STRING from DEGs exclusive to the mixture treatment (Fig. 5) indicate changes to molecular networks associated to metabolic processes. This includes the response to xenobiotic, with up-regulation of Cyp26a1and Cyp3a65 during phase I (biotransformation) and concomitant up-regulation of Ugt1a1 and Ugt5a2 involved in glucuronidation (phase II). Two short-chain dehydrogenases/reductases (SDRs) were also linked to Cyp26a1, but their activity was suppressed by exposure to the mixture. The mitogen-activated protein kinase (MAPK) pathway, highlighted by up-regulation of Jun oncoprotein and Mapk12b (which enables MAPK activity), which can be associated to the regulation of apoptosis and cell proliferation. Ubiquitination, protein homeostasis, oxidative stress response and cholesterol metabolism were mainly potentiated by

Table 3
Canonical KEGG pathway analysis. Gene enrichment analysis was done with all genes identified in the transcriptomes of zebrafish embryos exposed to B[*a*]P, DFC and the mixture of the two contaminants.

	KEGG Pathway	FDR-adjusted p[a]	NES[b]	size
B[*a*]P	Tryptophan metabolism	4.56×10^{-3}	2.323818	52
	Steroid hormone biosynthesis	5.26×10^{-3}	2.372632	69
	Metabolism of xenobiotics by cytochrome P450	2.59×10^{-2}	2.513161	61
DFC	MAPK signalling pathway	3.39×10^{-5}	1.927695	397
	Cytokine-cytokine receptor interaction	9.59×10^{-3}	1.808769	184
	Apoptosis	1.16×10^{-2}	1.90573	172
	Herpes simplex virus 1 infection	1.16×10^{-2}	1.776337	165
	NOD-like receptor signalling pathway	1.75×10^{-2}	1.859701	134
	Adipocytokine signalling pathway	1.86×10^{-2}	1.909814	82
	RNA degradation	2.93×10^{-2}	1.769055	16
	Toll-like receptor signalling pathway	2.93×10^{-2}	1.770994	99
	p53 signalling pathway	2.93×10^{-2}	1.946374	85
	VEGF signalling pathway	3.05×10^{-2}	1.816578	79
	FoxO signalling pathway	3.78×10^{-2}	1.63135	166
	Caffeine metabolism	3.83×10^{-2}	−1.56162	4
	Steroid biosynthesis	4.46×10^{-2}	1.710755	22
Mixture	MAPK signalling pathway	2.27×10^{-4}	1.895394	397
	Apoptosis	2.35×10^{-3}	2.031882	172
	Metabolism of xenobiotics by cytochrome P450	3.96×10^{-3}	2.065028	61
	Toll-like receptor signalling pathway	1.73×10^{-2}	1.833873	99
	NOD-like receptor signalling pathway	1.73×10^{-2}	1.861289	134
	Herpes simplex virus 1 infection	1.73×10^{-2}	1.77273	165
	p53 signalling pathway	1.73×10^{-2}	2.009452	85
	Steroid hormone biosynthesis	1.73×10^{-2}	1.989381	69
	Adipocytokine signalling pathway	3.37×10^{-2}	1.909841	82

[a] Through FGSEA analysis.
[b] Normalised enrichment score.

exposure to the mixed toxicants according. Additionally, two pairs of up- and down-regulated proteins (respectively) revealed a possible interference in eye and lens development (Cryaa, Hsf4) and sexual maturation (Zpcx, Paqr5a).

4. Discussion

The current work explored the potential interactions between realistic mixtures of B[*a*]P and DFC, which are representative models of legacy and emerging contaminants, respectively, taking the *in vivo* zebrafish embryo as biological model. Transcriptomics revealed ~300 DEGs that were exclusive of the mixture treatment. Gene ontology revealed deactivation of biological processes and molecular functions linked to eye development or function and activation of molecular heterodimerization activity in embryos co-exposed to B[*a*]P and DFC, which overall suggests a synergistic interaction. However, the loss of relative enrichment significance of pathways that were relevant in embryos exposed to single toxicants, namely those associated to RNA degradation, cell proliferation, apoptosis and cell-cycle control can indicate antagonistic interaction. These findings imply a cautionary tale when suggesting that some specific toxicopathic outcomes result from synergism or antagonism since further analysis should be necessary to determine the implications of these changes in zebrafish growth, health and reproduction. Altogether, this means that interaction effects must be analysed and interpreted by integrating molecular mechanism with toxicopathic effects. Degradation of RNA, for instance, is a paramount and complex cellular function. Its deregulation can lead to the accumulation of defective RNAs or intermediates, with severe consequences for the regulation of gene expression (Houseley and Tollervey, 2009). We may hypothesize that reduced significance of this pathway in zebrafish embryos subjected to the mixture treatment can be linked to reduced expression in some of the top five genes involved in transcription and translation, such as *znf143b* and *eif2b2*, respectively.

One of the most significant crosslinks between toxicopathic effects and molecular mechanism concerns the formation of heart cavity and yolk sac oedemas in embryos from exposure to DFC isolated or combined. This adverse outcome (AO) follows key events (KE) associated with the regulation of ribosomal proteins with p53 function, thus leading to hindered cell cycle arrest and apoptosis, which is a vital procedure when DNA quality is compromised beyond repair, therefore potentiating mutagenesis and teratogenesis. More than 50% of all DEGs retrieved from the mixture treatment were in common with those isolated from the DFC-only exposure, which uncovered the high influence of DFC exposure in mixture. Among the most overexpressed genes from this subset, we found *rpl32* (exposure to DFC) and *rpl21* (mixture treatment). These genes encode for ribosomal proteins and are involved in translation. However, the resulting proteins have both been linked to cancer progression and metastasis development via degradation of p53 and activation of the FAK/paxillin/ERK signalling pathway (Xie et al., 2020; Zhu et al., 2023). Moreover, DFC and mixture treatments shared the underexpressed genes *cuedc1a* and *ddb2*, both linked to DNA repair and protein ubiquitination, that may also have implications for the p53-related apoptosis pathways, as inferred from GE analysis. It should be noted that DNA damage was significantly increased in embryos exposed to B[*a*]P and mixture treatments but not in DFC, which suggests that alterations to p53 regulation may not be related with molecular initiating event (MIE) as DNA damage caused by exposure to the NSAID. In fact, DFC was considered not genotoxic either *in vivo* or *in vitro* assays by Hartmann et al. (2021), although Gómez-Oliván et al. (2014) registered significant DNA damage in *Daphnia magna* after 48-h exposure to 9.7 mg/L, which is ten times higher than the concentration tested in this study. Additionally, in animals exposed to DFC and mixtures, we found the activation of biological process 'DNA replication' and the molecular function 'DNA binding', which added to the alterations mentioned suggest an investment in cellular proliferation that may be connected to hindered cell cycle arrest and onset of apoptosis that may not necessarily be linked to genotoxicity. Nonetheless, these findings are at this point conjectural and need further enhancement, with emphasis on the presence of ROS and overall role of oxidative stress in the process. In addition, it must also be safeguarded that the effects and responses of the (whole-body) zebrafish embryo may differ from the organs and systems of fully developed animals.

According to Brown and Benchimol (2006), the p53-mediated apoptotic cascade and cell cycle arrest can be activated or deactivated depending on the progression of mitogen-activated protein kinase (MAPK) pathway. Indeed, we must recall that the GSEA results from DFC and mixture-exposed embryos indicated significant alterations in this pathway. In turn, protein-protein interaction networks associated to overexpressed genes in embryos subjected to the mixture treatment (see Fig. 5) also suggest activation of the MAPK pathway. It must also be noted that despite the reduced genotoxicity of DFC, this compound can induce intracellular reactive oxygen species (ROS) and mitochondrial dysfunction, which can also generate ROS (Jung et al., 2020; Thai et al., 2023). This causes inflammation, with secretion of pro-inflammatory cytokines and growth factors that can stimulate the MAPK/ERK/Raf pathway (Manzoor and Koh, 2012; Mittal et al., 2014). This pathway leads to further inflammation, cell growth, cell proliferation and apoptosis. It should be noted that the ERK pathway was significantly altered in DFC and mixture treatments and that there are indications of activation of inflammatory and oxidative stress response in embryos subjected to mixed toxicants. Finally, an association can be made between the inflammatory cascade to and the formation of oedemas, which may result from the overpromotion of vascular permeability by pro-inflammatory molecules (Teixeira and Faria, 2021), and increased mortality in embryos exposed to DFC, isolated or combined with B[*a*]P.

Embryos co-exposed to DFC and B[*a*]P revealed another potential

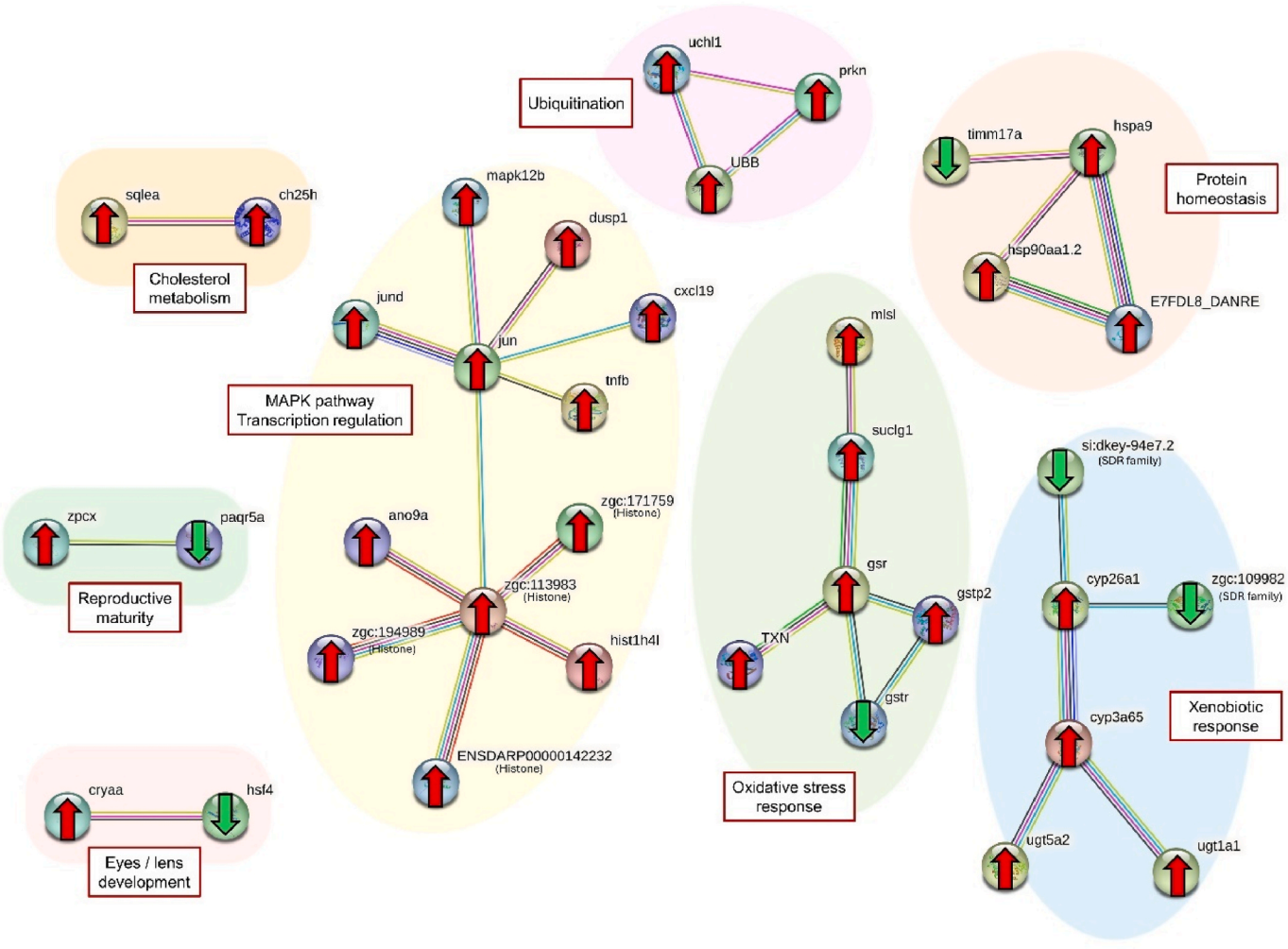

Fig. 5. Protein-protein interaction network retrieved using STRING from the translated open reading frames (ORFs) whole-transcriptomes of zebrafish embryos exposed to mixture of B[*a*]P and DFC. The networks were reconstructed from deferentially expressed genes exclusive to the mixture treatment. Red and green arrows means that protein is upregulated and downregulated, respectively. (For interpretation of the references to colour in this figure legend, the reader is referred to the Web version of this article.)

AO. Impaired ocular function be linked to eye degeneration (recall Fig. 1F) in exposed animals. Previous research on zebrafish eye development (see Dahm et al., 2007; Schmitt and Dowling, 1994) discard the scenario of developmental delay since the affected eyes retain a pigment layer and an individualized lens protruding from the optic cup, both of which visible after 84 hpf, as expected. Ocular dysfunction thus results from degeneration, which may involve repression of *cryaa* (Alfa-A--crystallin) and *hsf4* (heat shock transcription factor 4) genes, as inferred from protein-protein interactions using STRING (recall Fig. 5). These genes are paramount for lens development and maintenance (Fujimoto et al., 2004; Zou et al., 2015). In addition, repression of the expression of either or both genes, *hsf4* and *cryaa*, have been connected to problems such as cataracts and protein inclusions in lenses in humans and zebrafish (Fujimoto et al., 2004; M. Gao et al., 2017; Su et al., 2012). Nonetheless, eye degeneration was also noted in embryos subjected to DFC-only treatments, where genes *cryaa* and *hsp4* were not significantly underexpressed, which may suggest that this AO can the triggered by different molecular processes. In the future, it would be interesting to analyse and compare this potential AO in developing and fully developed animals exposed to mixtures of the toxicants.

Molecular mechanisms behind acute effects are difficult to trace due to complex series of molecular events occurring in a relatively short period. As such, some pathological alterations have only been associated to the concentrations of each substance. For example, embryos exposed to highest concentrations of DFC (1.3 and 2.5 μM), individually or mixed endured the highest development alteration rates. Severe alterations in zebrafish embryos caused by exposure to high DFC concentrations, namely reduced body size, smaller eyes, muscle degeneration, pericardial and body oedema, as well as abnormal pigmentation, had already reported by Chen et al. (2014); however, only at concentrations above 3.38 μM. Also, this same study reported 35% embryo lethality caused by this concentration, which contrasts with the 70% mortality recorded in the present study for low DFC concentrations (2.5 μM). This discrepancy can be explained, nonetheless, by the removal of the chorion, which is an important barrier against chemical agents (Henn and Braunbeck, 2011). Still, statistical modelling evidenced loss of DFC influence in both mortality and pathological alterations when mixed with B[*a*]P. In turn, the reduced acute effects following exposure to B[*a*]P, isolated or combined, can be explained by the essentially chronic nature of effects caused by B[*a*]P, as opposed to DFC, which is known to cause high acute toxicity. Lin et al. (2020) observed neurotoxic effects, with alterations in nervous system development in zebrafish embryos exposed to B[*a*]P concentrations (10 and 20 μM) even higher than those used in this study, without any apparent morphological alteration. Despite this, embryos exposed to B[*a*]P at highest concentration (0.4 μM) revealed more DNA damage than for the DFC-only treatment. Interestingly, exposure to the mixture yielded similar DNA damage than exposure to B[*a*]P, therefore lower than the expected sum of genotoxic effects caused by the

toxicants, which suggests some form of antagonism. It must be emphasised that B[*a*]P is a known genotoxic agent even at relatively low concentrations. This has been described before in zebrafish embryos exposed to B[*a*]P for 6 days to concentrations of 0.001 μM and 0.01 μM (Šrut et al., 2015). Similarly, significant DNA damage occurred in *Oryzias latipes* embryos after 48 h exposure to 20 μg/L (Dasgupta et al., 2014), which corresponds to about one-third of the B[*a*]P concentration used in our study (89 μg/L). It must be noted that the genotoxicity of B[*a*]P derives in big part from DNA adducts formed after B[*a*]P bioactivation by CYP450 during phase I leading to the formation of highly reactive B[*a*]P diol-epoxides (Tarantini et al., 2009). Indeed, the metabolism of xenobiotics by CYP450 emerged as one of the pathways significantly affected by B[*a*]P, isolated or combined.

5. Conclusions

From pathological effects and potential toxicological mechanisms in zebrafish embryos exposed to combined DFC and B[*a*]P two potential AOPs may be suggested for further investigation in vertebrates exposed to these toxicants during early life stages and potentially in fully developed organs and systems of adults. One is linked to eye development and another to inflammation, cell cycle arrest and apoptosis via p53 and MAPK pathways. In either case, DFC, a poor genotoxicant, was found to be responsible for significant acute toxicopathic effects such as mortality and developmental malformation, even though the role of oxidative stress, although plausible, remains to be fully ascertained. The findings suggest a potential antagonistic interaction under the present circumstances of assessment onto genotoxicity and a few molecular pathways associated to cell cycle turnover and even apoptosis. We must highlight that B[*a*]P tends to cause serious chronic effects regardless of interaction effects, which means that the full span of consequences can only be understood after analysing the whole zebrafish life cycle.

CRediT authorship contribution statement

Carla Martins: Writing – original draft, Methodology, Investigation, Formal analysis, Conceptualization. **Lara M. Carvalho:** Methodology, Investigation. **Inês Moutinho Cabral:** Writing – review & editing, Software, Formal analysis. **Leonor Saúde:** Writing – review & editing, Resources. **Kristian Dreij:** Writing – review & editing, Supervision. **Pedro M. Costa:** Writing – review & editing, Supervision, Resources, Methodology, Conceptualization.

Ethics statement

The present work deployed embryonic organisms (zebrafish) only, compliant with the 'Three R' policy. As per Directive 2010/63/EU, specific authorisation for animal testing is therefore waived.

Declaration of Competing Interest

The authors declare that they have no known competing financial interests or personal relationships that could have appeared to influence the work reported in this paper.

Acknowledgements

The Portuguese Foundation for Science and Technology (FCT) funded the grant SFRH/BD/120030/2016 to C.M. This work was also financed by the National Funds from FCT in the scope of the project UIDP/04378/2020 and UIDB/04378/2020 of the Research Unit on Applied Molecular Biosciences – UCIBIO and the project LA/P/0140/2020 of the Associate Laboratory Institute for Health and Bioeconomy – i4HB. We are also thankful to C. Gonçalves and M. D'Ambrosio (UCIBIO) for assistance with the Comet assay protocol.

Appendix A. Supplementary data

Supplementary data to this article can be found online at https://doi.org/10.1016/j.envpol.2024.125189.

Data availability

The accession to rawdata is provided in the text.

References

Ablain, J., Zon, L.I., 2013. Of fish and men: using zebrafish to fight human diseases. Trends Cell Biol. 23, 584–586. https://doi.org/10.1016/j.tcb.2013.09.009.

Ankley, G.T., Bennett, R.S., Erickson, R.J., Hoff, D.J., Hornung, M.W., Johnson, R.D., Mount, D.R., Nichols, J.W., Russom, C.L., Schmieder, P.K., Serrrano, J.A., Tietge, J. E., Villeneuve, D.L., 2010. Adverse outcome pathways: a conceptual framework to support ecotoxicology research and risk assessment. Environ. Toxicol. Chem. 29, 730–741. https://doi.org/10.1002/etc.34.

Arisan, E.D., Ergül, Z., Bozdağ, G., Rencüzoğulları, Ö., Çoker-Gürkan, A., Obakan-Yerlikaya, P., Coşkun, D., Palavan-Ünsal, N., 2018. Diclofenac induced apoptosis via altering PI3K/Akt/MAPK signaling axis in HCT 116 more efficiently compared to SW480 colon +cancer cells. Mol. Biol. Rep. 45, 2175–2184. https://doi.org/10.1007/s11033-018-4378-2.

Arman, N.Z., Salmiati, S., Aris, A., Salim, M.R., Nazifa, T.H., Muhamad, M.S., Marpongahtun, M., 2021. A review on emerging pollutants in the water environment: existences, health effects and treatment processes. Water 13, 1–31. https://doi.org/10.3390/w13223258.

Ashfaq, M., Nawaz Khan, K., Saif Ur Rehman, M., Mustafa, G., Faizan Nazar, M., Sun, Q., Iqbal, J., Mulla, S.I., Yu, C.P., 2017. Ecological risk assessment of pharmaceuticals in the receiving environment of pharmaceutical wastewater in Pakistan. Ecotoxicol. Environ. Saf. 136, 31–39. https://doi.org/10.1016/j.ecoenv.2016.10.029.

Azqueta, A., Collins, A.R., 2013. The essential comet assay: a comprehensive guide to measuring DNA damage and repair. Arch. Toxicol. 87, 949–968. https://doi.org/10.1007/s00204-013-1070-0.

Boström, C.E., Gerde, P., Hanberg, A., Jernström, B., Johansson, C., Kyrklund, T., Rannug, A., Törnqvist, M., Victorin, K., Westerholm, R., 2002. Cancer risk assessment, indicators, and guidelines for polycyclic aromatic hydrocarbons in the ambient air. Environ. Health Perspect. 110, 451–488. https://doi.org/10.1289/ehp.110-1241197.

Bray, N.L., Pimentel, H., Melsted, P., Pachter, L., 2016. Near-optimal probabilistic RNA-seq quantification. Nat. Biotechnol. 34, 525–527. https://doi.org/10.1038/nbt.3519.

Brown, L., Benchimol, S., 2006. The involvement of MAPK signaling pathways in determining the cellular response to p53 activation. J. Biol. Chem. 281, 3832–3840. https://doi.org/10.1074/jbc.M507951200.

Canzler, S., Hackermüller, J., 2020. multiGSEA: a GSEA-based pathway enrichment analysis for multi-omics data. BMC Bioinform 21, 1–13. https://doi.org/10.1186/s12859-020-03910-x.

Carlson, M., 2019. org.Dr.eg.db: genome wide annotation for Zebrafish. R package version 3.8.2.

Cassee, F.R., Groten, J.P., Van Bladeren, P.J., Feron, V.J., 1998. Toxicological evaluation and risk assessment of chemical mixtures. Crit. Rev. Toxicol. 28, 73–101. https://doi.org/10.1080/10408449891344164.

Chahardehi, A.M., Arsad, H., Lim, V., 2020. Zebrafish as a successful animal model for screening toxicity of medicinal plants. Plants 9, 1345. https://doi.org/10.3390/plants9101345.

Chen, J. Bin, Gao, H.W., Zhang, Y.L., Zhang, Y., Zhou, X.F., Li, C.Q., Gao, H.P., 2014. Developmental toxicity of diclofenac and elucidation of gene regulation in zebrafish (*Danio rerio*). Sci. Rep. 4, 1–7. https://doi.org/10.1038/srep04841.

Costa, P.M., 2022. Current aspects of DNA damage and repair in ecotoxicology: a mini-review. Ecotoxicology 31, 1–11. https://doi.org/10.1007/s10646-021-02487-2.

Dahm, R., Schonthaler, H.B., Soehn, A.S., van Marle, J., Vrensen, G.F.J.M., 2007. Development and adult morphology of the eye lens in the zebrafish. Exp. Eye Res. 85, 74–89. https://doi.org/10.1016/j.exer.2007.02.015.

Dasgupta, S., Cao, A., Mauer, B., Yan, B., Uno, S., McElroy, A., 2014. Genotoxicity of oxy-PAHs to Japanese medaka (*Oryzias latipes*) embryos assessed using the comet assay. Environ. Sci. Pollut. Res. 21, 13867–13876. https://doi.org/10.1007/s11356-014-2586-4.

Dat, N.D., Chang, M.B., 2017. Review on characteristics of PAHs in atmosphere, anthropogenic sources and control technologies. Sci. Total Environ. 609, 682–693. https://doi.org/10.1016/j.scitotenv.2017.07.204.

Denissenko, M.F., Pao, A., Tang, M.S., Pfeifer, G.P., 1996. Preferential formation of benzo [a]pyrene adducts at lung cancer mutational hotspots in P53. Science 274, 430–432. https://doi.org/10.1126/science.274.5286.430.

Diniz, M.S., Salgado, R., Pereira, V.J., Carvalho, G., Oehmen, A., Reis, M.A.M., Noronha, J.P., 2015. Ecotoxicity of ketoprofen, diclofenac, atenolol and their photolysis byproducts in zebrafish (*Danio rerio*). Sci. Total Environ. 505, 282–289. https://doi.org/10.1016/j.scitotenv.2014.09.103.

Durinck, S., Spellman, P.T., Birney, E., Huber, W., 2009. Mapping identifiers for the integration of genomic datasets with the R/Bioconductor package biomaRt. Nat. Protoc. 4, 1184–1191. https://doi.org/10.1038/nprot.2009.97.

Duval, A.P., Troquier, L., Silva, O.D.S., Demartines, N., Dormond, O., 2019. Diclofenac potentiates sorafenib-based treatments of hepatocellular carcinoma by enhancing oxidative stress. Cancers 11, 1453. https://doi.org/10.3390/cancers11101453.

Ferrari, B., Paxéus, N., Giudice, R. lo, Pollio, A., Garric, J., 2003. Ecotoxicological impact of pharmaceuticals found in treated wastewaters: study of carbamazepine, clofibric acid, and diclofenac. Ecotoxicol. Environ. Saf. 55, 359–370. https://doi.org/10.1016/S0147-6513(02)00082-9.

Fujimoto, M., Izu, H., Seki, K., Fukuda, K., Nishida, T., Yamada, S., Kato, K., Yonemura, S., Inouye, S., Nakai, A., 2004. HSF4 is required for normal cell growth and differentiation during mouse lens development. EMBO J. 23, 4297–4306. https://doi.org/10.1038/sj.emboj.7600435.

Gao, D., Wang, C., Xi, Z., Zhou, Y., Wang, Y., Zuo, Z., 2017a. Early-life benzo[a]pyrene exposure causes neurodegenerative syndromes in adult zebrafish (*Danio rerio*) and the mechanism involved. Toxicol. Sci. 157, 74–84. https://doi.org/10.1093/toxsci/kfx028.

Gan, T.J., 2010. Diclofenac: an update on its mechanism of action and safety profile. Curr. Med. Res. Opin. 26, 1715–1731. https://doi.org/10.1185/03007995.2010.486301.

Gao, M., Huang, Y., Wang, L., Huang, M., Liu, F., Liao, S., Yu, S., Lu, Z., Han, S., Hu, X., Qu, Z., Liu, X., Assefa Yimer, T., Yang, L., Tang, Z., Li, D.W.-C., Liu, M., 2017b. HSF4 regulates lens fiber cell differentiation by activating p53 and its downstream regulators. Cell Death Dis. 8. https://doi.org/10.1038/cddis.2017.478, 3082–e3082.

Gómez-Oliván, L.M., Galar-Martínez, M., García-Medina, S., Valdés-Alanís, A., Islas-Flores, H., Neri-Cruz, N., 2014. Genotoxic response and oxidative stress induced by diclofenac, ibuprofen and naproxen in *Daphnia magna*. Drug Chem. Toxicol. 37, 391–399. https://doi.org/10.3109/01480545.2013.870191.

Gonzalez-Rey, M., Bebianno, M.J., 2014. Effects of non-steroidal anti-inflammatory drug (NSAID) diclofenac exposure in mussel *Mytilus galloprovincialis*. Aquat. Toxicol. 148, 818–831. https://doi.org/10.1016/j.aquatox.2014.01.011.

Guerreiro, C.B.B., Horálek, J., de Leeuw, F., Couvidat, F., 2016. Benzo(a)pyrene in Europe: ambient air concentrations, population exposure and health effects. Environ Pollut 214, 657–667. https://doi.org/10.1016/j.envpol.2016.04.081.

Hartmann, A., Erkman, L., Maremanda, N., Elhajouji, A., Martus, H.J., 2021. Comprehensive review of genotoxicity data for diclofenac. Mutat. Res. Genet. Toxicol. Environ. Mutagen 866, 503347. https://doi.org/10.1016/j.mrgentox.2021.503347.

Hayes, A.W., Li, R., Hoeng, J., Iskandar, A., Peistch, M.C., Dourson, M.L., 2019. New approaches to risk assessment of chemical mixtures. Toxicol. Res. Appl. 3, 239784731882076. https://doi.org/10.1177/2397847318820768.

Heberer, T., 2002. Occurrence, fate, and removal of pharmaceutical residues in the aquatic environment: a review of recent research data. Toxicol. Lett. 131, 5–17. https://doi.org/10.1016/S0378-4274(02)00041-3.

Henn, K., Braunbeck, T., 2011. Dechorionation as a tool to improve the fish embryo toxicity test (FET) with the zebrafish (*Danio rerio*). Comparative Biochemistry and Physiology - C Toxicology and Pharmacology 153, 91–98. https://doi.org/10.1016/j.cbpc.2010.09.003.

Hernández, A.F., Gil, F., Lacasaña, M., 2017. Toxicological interactions of pesticide mixtures: an update. Arch. Toxicol. 91, 3211–3223. https://doi.org/10.1007/s00204-017-2043-5.

Howe, K., Clark, M.D., Torroja, C.F., Torrance, J., Berthelot, C., Muffato, M., Collins, J.E., 2013. The zebrafish reference genome sequence and its relationship to the human genome. Nature 496, 498–503. https://doi.org/10.1038/nature12111.

Houseley, J., Tollervey, D., 2009. The many pathways of RNA degradation. Cell 136, 763–776. https://doi.org/10.1016/j.cell.2009.01.019.

Ihaka, R., Gentleman, R., 1996. R: a language for data analysis and graphics. J. Comput. Graph Stat. 5, 299–314. https://doi.org/10.1080/10618600.1996.10474713.

Inoue, A., Muranaka, S., Fujita, H., Kanno, T., Tamai, H., Utsumi, K., 2004. Molecular mechanism of diclofenac-induced apoptosis of promyelocytic leukemia: dependency on reactive oxygen species, Akt, Bid, cytochrome c, and caspase pathway. Free Rad Biol Med 37, 1290–1299. https://doi.org/10.1016/j.freeradbiomed.2004.07.003.

Jung, S.H., Lee, W., Park, S.H., Lee, K.Y., Choi, Y.J., Choi, S., Kang, D., Kim, S., Chang, T. S., Hong, S.S., Lee, B.H., 2020. Diclofenac impairs autophagic flux via oxidative stress and lysosomal dysfunction: implications for hepatotoxicity. Redox Biol. 37, 101751. https://doi.org/10.1016/j.redox.2020.101751.

Kaur, J., Sanyal, S.N., 2011. Diclofenac, a selective COX-2 inhibitor, inhibits DMH-induced colon tumorigenesis through suppression of MCP-1, MIP-1α and VEGF. Mol. Carcinog. 50, 707–718. https://doi.org/10.1002/mc.20736.

Knecht, A.L., Truong, L., Simonich, M.T., Tanguay, R.L., 2017. Developmental benzo[a]pyrene (B[a]P) exposure impacts larval behavior and impairs adult learning in zebrafish. Neurotoxicol. Teratol. 59, 27–34. https://doi.org/10.1016/j.ntt.2016.10.006.

Kumar, S., Stecher, G., Li, M., Knyaz, C., Tamura, K., 2018. Mega X: molecular evolutionary genetics analysis across computing platforms. Mol. Biol. Evol. 35, 1547–1549. https://doi.org/10.1093/molbev/msy096.

Leemann, T., Transon, C., Dayer, P., 1993. Cytochrome P450TB (CYP2C): a major monooxygenase catalyzing diclofenac 4′-hydroxylation in human liver. Life Sci. 52, 29–34. https://doi.org/10.1016/0024-3205(93)90285-B.

Lin, Y.C., Wu, C.Y., Hu, C.H., Pai, T.W., Chen, Y.R., Wang, W.D., 2020. Integrated hypoxia signaling and oxidative stress in developmental neurotoxicity of benzo[a]pyrene in zebrafish embryos. Antioxidants 9, 1–71. https://doi.org/10.3390/antiox9080731.

Livak, K.J., Schmittgen, T.D., 2001. Analysis of relative gene expression data using real-time quantitative PCR and the 2-ΔΔCT method. Methods 25, 402–408. https://doi.org/10.1006/meth.2001.1262.

Luft, J.H., 1961. Improvements in epoxy resin embedding methods. J. Biophys. Biochem. Cytol. 9, 409–414. https://doi.org/10.1083/jcb.9.2.409.

Madeira, C., Costa, P.M., 2021. Proteomics in Systems Toxicology, pp. 55–91. https://doi.org/10.1016/bs.apcsb.2021.03.001.

Maes, J., Verlooy, L., Buenafe, O.E., de Witte, P.A.M., Esguerra, C.V., Crawford, A.D., 2012. Evaluation of 14 organic solvents and carriers for screening applications in zebrafish embryos and larvae. PLoS One 7, 1–9. https://doi.org/10.1371/journal.pone.0043850.

Manoli, E., Samara, C., 1999. Polycyclic aromatic hydrocarbons in natural waters: sources, occurrence and analysis. TrAC, Trends Anal. Chem. 18, 417–428. https://doi.org/10.1016/S0165-9936(99)00111-9.

Manzoor, Z., Koh, Y.-S., 2012. Mitogen-activated protein kinases in inflammation. J. Bacteriol. Virol. 42, 189. https://doi.org/10.4167/jbv.2012.42.3.189.

Martins, C., Costa, P.M., 2020. Technical updates to the comet assay in vivo for assessing DNA damage in zebrafish embryos from fresh and frozen cell suspensions. Zebrafish 1–9. https://doi.org/10.1089/zeb.2020.1857, 00.

Martins, C., Dreij, K., Costa, P.M., 2019. The state-of-the art of environmental toxicogenomics: challenges and perspectives of "omics" approaches directed to toxicant mixtures. Int J Environ Res Public Health 16, 1–16. https://doi.org/10.3390/ijerph16234718.

McCarthy, D.J., Chen, Y., Smyth, G.K., 2012. Differential expression analysis of multifactor RNA-Seq experiments with respect to biological variation. Nucleic Acids Res. 40, 4288–4297. https://doi.org/10.1093/nar/gks042.

McCullagh, P., Nelder, J., 1989. Generalized Linear Models, second ed., Second. Chapman & Hall/CRC.

Mittal, M., Siddiqui, M.R., Tran, K., Reddy, S.P., Malik, A.B., 2014. Reactive oxygen species in inflammation and tissue injury. Antioxid Redox Signal 20, 1126–1167. https://doi.org/10.1089/ars.2012.5149.

Oaks, J.L., Gilbert, M., Virani, M.Z., Watson, R.T., Meteyer, C.U., Rideout, B.A., Shivaprasad, H.L., Ahmed, S., Chaudhry, M.J.I., Arshad, M., Mahmood, S., Ali, A., Khan, A.A., 2004. Diclofenac residues as the cause of vulture population decline in Pakistan. Nature 427, 630–633. https://doi.org/10.1038/nature02317.

OECD (Organisation for Economic Co-operation and Development), 2013. OECD Guidelines for the Testing of Chemicals 1–22.

Parolini, M., 2020. Toxicity of the non-steroidal anti-inflammatory drugs (NSAIDs) acetylsalicylic acid, paracetamol, diclofenac, ibuprofen and naproxen towards freshwater invertebrates: a review. Sci. Total Environ. 740, 140043. https://doi.org/10.1016/j.scitotenv.2020.140043.

Ritchie, M.E., Phipson, B., Wu, D., Hu, Y., Law, C.W., Shi, W., Smyth, G.K., 2015. Limma powers differential expression analyses for RNA-sequencing and microarray studies. Nucleic Acids Res. 43, e47. https://doi.org/10.1093/nar/gkv007.

Robinson, M.D., McCarthy, D.J., Smyth, G.K., 2009. edgeR: a Bioconductor package for differential expression analysis of digital gene expression data. Bioinformatics 26, 139–140. https://doi.org/10.1093/bioinformatics/btp616.

Ross, J.A., Nesnow, S., 1999. Polycyclic aromatic hydrocarbons: correlations between DNA adducts and ras oncogene mutations. Mutation Research - Fundamental and Molecular Mechanisms of Mutagenesis 424, 155–166. https://doi.org/10.1016/S0027-5107(99)00016-0.

Schmitt, E.A., Dowling, J.E., 1994. Early-eye morphogenesis in the zebrafish, Brachydanio rerio. J. Comp. Neurol. 344, 532–542. https://doi.org/10.1002/cne.903440404.

Schroeder, A., Mueller, O., Stocker, S., Salowsky, R., Leiber, M., Gassmann, M., Lightfoot, S., Menzel, W., Granzow, M., Ragg, T., 2006. The RIN: an RNA integrity number for assigning integrity values to RNA measurements. BMC Mol. Biol. 7, 1–14. https://doi.org/10.1186/1471-2199-7-3.

Silins, I., Högberg, J., 2011. Combined toxic exposures and human health: biomarkers of exposure and effect. Int J Environ Res Public Health 8, 629–647. https://doi.org/10.3390/ijerph8030629.

Singh, N.P., Mccoy, M.T., Tice, R.R., Scineider, E.L., 1988. A simple technique for quantification of low levels of DNA in individual cells. Exp. Cell Res. 175, 184–191. https://doi.org/10.1016/0014-4827(88)90265-0.

Šrut, M., Štambuk, A., Bourdineaud, J.-P., Klobučar, G.I.V., 2015. Zebrafish genome instability after exposure to model genotoxicants. Ecotoxicology 24, 887–902. https://doi.org/10.1007/s10646-015-1432-x.

Su, D., Guo, Y., Li, Q., Guan, L., Zhu, S., Ma, X., 2012. A novel mutation in CRYAA is associated with autosomal dominant suture cataracts in a Chinese family. Mol. Vis. 18, 3057–3063.

Szklarczyk, D., Gable, A.L., Lyon, D., Junge, A., Wyder, S., Huerta-Cepas, J., Simonovic, M., Doncheva, N.T., Morris, J.H., Bork, P., Jensen, L.J., Von Mering, C., 2019. STRING v11: protein-protein association networks with increased coverage, supporting functional discovery in genome-wide experimental datasets. Nucleic Acids Res. 47, D607–D613. https://doi.org/10.1093/nar/gky1131.

Tarantini, A., Maitre, A., Lefebvre, E., Marques, M., Marie, C., Ravanat, J.L., Douki, T., 2009. Relative contribution of DNA strand breaks and DNA adducts to the genotoxicity of benzo[a]pyrene as a pure compound and in complex mixtures. Mutation Research - Fundamental and Molecular Mechanisms of Mutagenesis 671, 67–75. https://doi.org/10.1016/j.mrfmmm.2009.08.014.

Teixeira, G., Faria, R., 2021. Inflammatory mediators leading to edema formation through plasma membrane receptors. In: Infections and Sepsis Development. IntechOpen. https://doi.org/10.5772/intechopen.99230.

Thai, P.N., Ren, L., Xu, W., Overton, J., Timofeyev, V., Nader, C.E., Haddad, M., Yang, J., Gomes, A.V., Hammock, B.D., Chiamvimonvat, N., Sirish, P., 2023. Chronic diclofenac exposure increases mitochondrial oxidative stress, inflammatory mediators, and cardiac dysfunction. Cardiovasc. Drugs Ther. 37, 25–37. https://doi.org/10.1007/s10557-021-07253-4.

Verlicchi, P., al Aukidy, M., Zambello, E., 2012. Occurrence of pharmaceutical compounds in urban wastewater: removal, mass load and environmental risk after a

secondary treatment-A review. Sci. Total Environ. 429, 123–155. https://doi.org/10.1016/j.scitotenv.2012.04.028.

Vitorino, J.D., Costa, P.M., 2023. After a century of research into environmental mutagens and carcinogens, where do we stand? Int J Environ Res Public Health 20, 1040. https://doi.org/10.3390/ijerph20021040.

Vystavna, Y., Frkova, Z., Celle-Jeanton, H., Diadin, D., Huneau, F., Steinmann, M., Crini, N., Loup, C., 2018. Priority substances and emerging pollutants in urban rivers in Ukraine: occurrence, fluxes and loading to transboundary European Union watersheds. Sci. Total Environ. 637–638, 1358–1362. https://doi.org/10.1016/j.scitotenv.2018.05.095.

Wu, X., Gao, X., Tan, T., Li, C., Yan, R., Chi, Z., Feng, Y., Gong, P., Fang, J., Zhang, X., Aihemaiti, K., Xu, D., 2021. Sources and pollution path identification of PAHs in karst aquifers: an example from Liulin karst water system, northern China. J. Contam. Hydrol. 241, 103810. https://doi.org/10.1016/j.jconhyd.2021.103810.

Xie, J., Zhang, W., Liang, X., Shuai, C., Zhou, Y., Pan, H., Yang, Y., Han, W., 2020. RPL32 promotes lung cancer progression by facilitating p53 degradation. Mol. Ther. Nucleic Acids 21, 75–85. https://doi.org/10.1016/j.omtn.2020.05.019.

Zhou, Y., Meng, J., Zhang, M., Chen, S., He, B., Zhao, H., Li, Q., Zhang, S., Wang, T., 2019. Which type of pollutants need to be controlled with priority in wastewater treatment plants: traditional or emerging pollutants? Environ. Int. 131. https://doi.org/10.1016/j.envint.2019.104982.

Zhu, J., Long, T., Gao, L., Zhong, Y., Wang, P., Wang, X., Li, Z., Hu, Z., 2023. RPL21 interacts with LAMP3 to promote colorectal cancer invasion and metastasis by regulating focal adhesion formation. Cell. Mol. Biol. Lett. 28, 31. https://doi.org/10.1186/s11658-023-00443-y.

Zou, P., Wu, S.-Y., Koteiche, H.A., Mishra, S., Levic, D.S., Knapik, E., Chen, W., Mchaourab, H.S., 2015. A conserved role of αA-crystallin in the development of the zebrafish embryonic lens. Exp. Eye Res. 138, 104–113. https://doi.org/10.1016/j.exer.2015.07.001.